Fast Neutral-Beam Photofragment Spectroscopy of H_2 $c\,^3\Pi_u^-$

H. Helm,[a] D. P. de Bruijn, and J. Los
FOM-Institute for Atomic and Molecular Physics, Kruislaan 407, 1098-SJ Amsterdam, The Netherlands
(Received 16 July 1984)

A time- and position-sensitive detector has been used for the first determination of the momentum distribution of correlated photofragments. A fast beam of H_2 $c\,^3\Pi_u^-$ is observed to undergo three types of photodissociation: (1) radiative dissociation of individual rovibrational levels; (2) predissociation by barrier tunneling of quasibound levels, for the first time observed in a neutral system with fragment energy analysis; and (3) direct photodissociation, which has been rotationally resolved for the first time.

PACS numbers: 33.80.Gj, 35.80.+s

We report a novel approach to the study of excited states of neutral molecules by photofragment spectroscopy. A fast beam of excited neutral molecules formed by near-resonant charge exchange is photodissociated with a tunable dye laser in a crossed-beam configuration and the resulting photofragments are detected with high efficiency with a time- and position-sensitive detector,[1,2] which allows measurement of the momentum distribution of fragment pairs arising from a single dissociation event.

A schematic diagram of the experimental arrangement is shown in Fig. 1. A velocity-analyzed beam of H_2^+, formed by electron-impact ionization of H_2 and accelerated to 7.5 keV, is directed through an alkali-metal vapor oven of 10 mm length. Near-resonant charge exchange of H_2^+ in alkali metals is known[3] to populate strongly the H_2 $c\,^3\Pi_u$ state. While the $c\,^3\Pi_u^+$ component decays rapidly by predissociation through the $b\,^3\Sigma_u^+$ state, the levels belonging to $c\,^3\Pi_u^-$ are long lived[4] ($\tau \sim 0.1$–1 ms). A pair of deflection plates allows

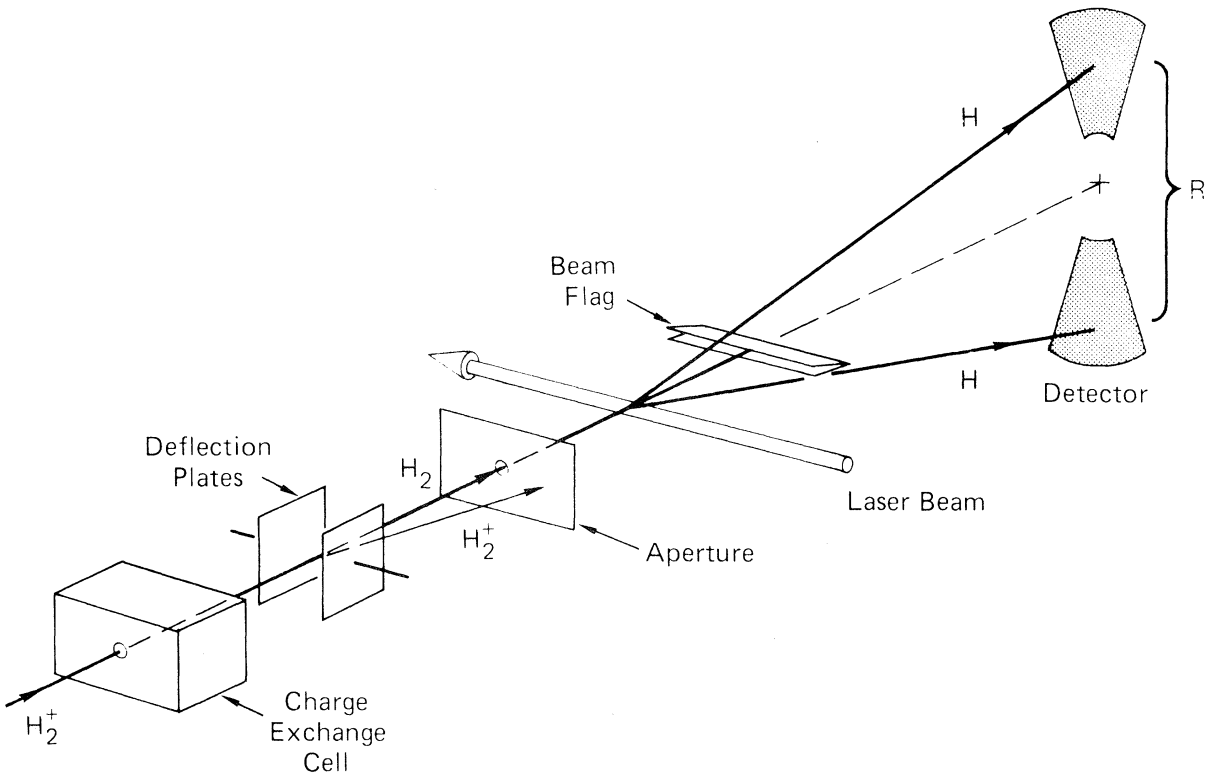

FIG. 1. Schematic diagram of the neutral-beam photofragment spectrometer with time- and position-sensitive detector. In the current experiments the laser polarization was set perpendicular to the plane of the neutral beam and laser beam.

separation of the remaining H_2^+ ions from the fast neutral beam. The neutral beam then enters a UHV chamber (pressure $\sim 4\times 10^{-9}$ Torr) through a 0.5-mm-diam aperture, is crossed with the intracavity beam of a cw dye-laser, and reaches a V-shaped beam flag which shadows the inactive portion of the position-sensitive detector which is located 154 cm from the photon interaction region.

The multichannel plate detector[1] consists of two opposing sectors of opening angle 20° which allow separate detection of the two photofragments produced in a single photodissociation event. The detector and its associated electronics permit the measurement of the spatial separation, R, of the two fragments at the channel-plate surface with a precision of typically 70 μm by measurement of the center of charge of each electron cloud emitted by the channel plates with a multianode system and the FOM charge division[1] method. The flight-time difference between these two fragments can be measured with a precision of 500 ps with the fast current pulse induced in the supply lines to the output face of the channel plates when a particle is detected. The spatial separation, R, that can be measured with the current device lies between 1 and 4 cm. At 7.5-keV parent-beam energy, this separation corresponds to c.m. energy releases in the range from 80 meV to 1.25 eV when dissociation occurs perpendicular to the parent-beam direction.

By tuning the dye laser and monitoring the coincidence count rate we obtain absorption spectra of transitions in the neutral beam which lead to photodissociation. Figure 2 shows an example of an absorption spectrum obtained with rhodamine 6G dye. For the strongest transitions, the coincidence counting rate reaches typically 10^4 fragment pairs/s with a primary beam current of H_2^+ of 10^{-10} A and a pressure in the charge-exchange cell of 10^{-3} Torr, for an intracavity laser power of 20 W. The linewidth of the transitions observed in Fig. 2 is limited by the linewidth of the multimode dye laser (~ 1 cm^{-1}).

Space- and time-resolved spectra of photofragment pairs were recorded with the dye laser set to a fixed wavelength. In the current paper we restrict our discussion to spatial spectra which are obtained for fragments with flight-time differences < 2 ns. Fragments with such small flight-time differences are formed when dissociation occurs very nearly perpendicular to the molecular-beam axis. Under these conditions the c.m. separation energy, W, is

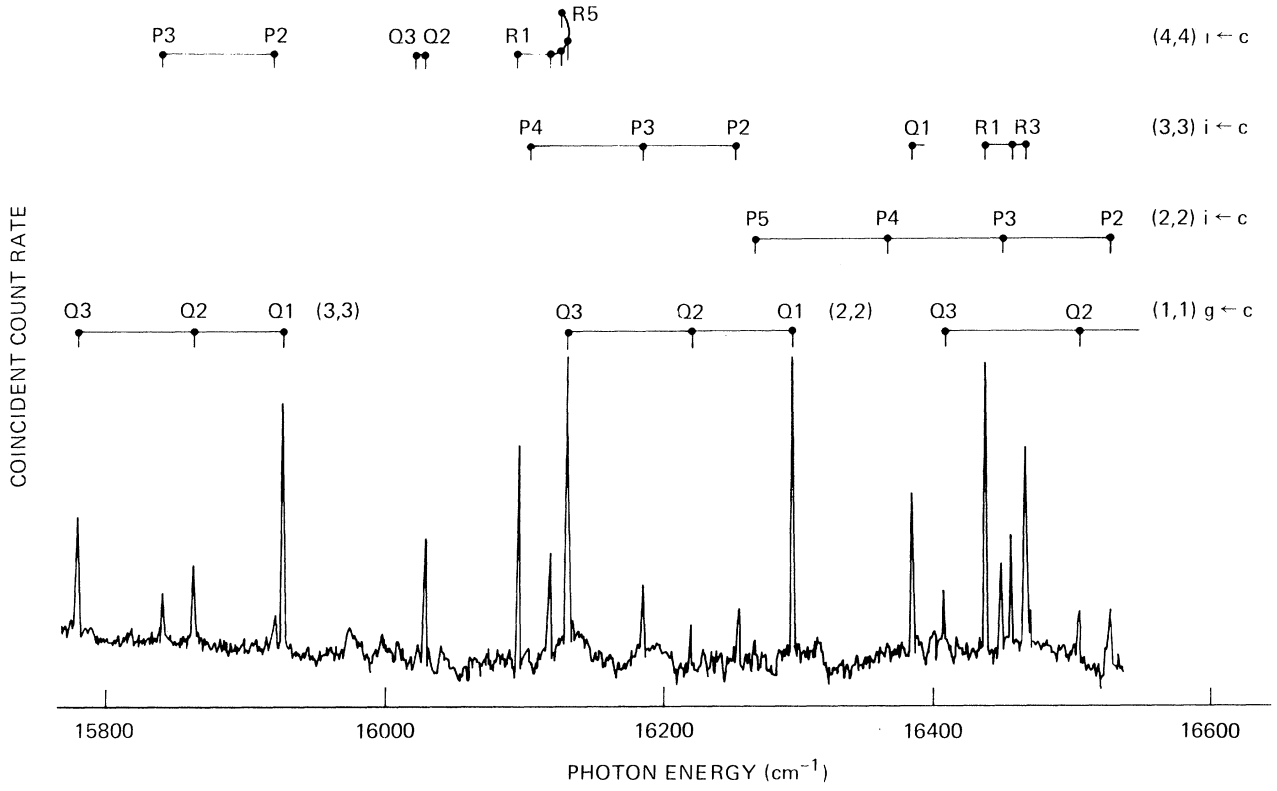

FIG. 2. Photodissociation spectrum of H_2 $c\,^3\Pi_u^-$.

related to the measured spatial separation of the photofragments, R, by the equation

$$W = E_0(R/L)^2, \quad (1)$$

where E_0 is the parent-beam energy and L is the distance from the photon interaction region to the detector.

In Fig. 3 we show spatial spectra which illustrate three different mechanisms of photodissociation that contribute to the spectrum in Fig. 2. Their origin may be understood with the help of Fig. 4 which illustrates three photodissociation processes of H_2 $c\,^3\Pi_u$ through excitation of the $i\,^3\Pi_g$ state.

(1) *Bound-bound-free photodissociation.*—The excitation of bound triplet gerade states from $c\,^3\Pi_u$ gives rise to radiation[5,6] into the continuum of the $b\,^3\Sigma_u^+$ state. It is evident from Fig. 4 that excitation of a single rovibrational level in the $i\,^3\Pi_g$ state will give rise to a continuum distribution of photofragment energies which reflects the overlap of the bound-state vibrational wave function with the continuum wave function of the $b\,^3\Sigma_u^+$ state.

A number of transitions observed in Fig. 2 were assigned to such bound-bound-free transitions belonging to the $i\,^3\Pi_g \leftarrow c\,^3\Pi_u$ and $g\,^3\Sigma_g^+ \leftarrow c\,^3\Pi_u$ systems.[7] Figure 3(a) shows an example of the continuous fragment-energy distribution which is obtained when we pump the $R1$ line of the $i \leftarrow c$ transition in the (3,3) band. The measured energy distribution represents the lower-energy portion of the total distribution produced, fragments with separation energies > 1.25 eV falling outside the current detection geometry and time window. The small structure which appears in the continuum energy distribution in Fig. 3(a) arises from an underlying bound-free photodissociation which is disucssed below.

(2) *Bound-quasibound photodissociation.*—Dissociation of a single quasibound level produces fragments with discrete separation energy, revealing the absolute location of the quasibound level with respect to the dissociation limit. Several transitions to quasibound levels appear in the absorption spectrum in Fig. 2, which we have assigned to the (4,4) band of the $i \leftarrow c$ system. To our knowledge these transitions have not been recorded previously. Figure 3(b) shows as an example the kinetic-energy spectrum of photofragments produced by pumping the $R1$ line of the (4,4) band ($W \sim 160$ meV). The potential-energy curve given by Kolos and Rychlewski[8] supports six vibrational levels, two of which lie above the asymptotic dissociation limit $H(1s) + H(2p)$. The levels $v = 4$ and 5 are thus quasibound. We have calculated the tunneling lifetime to be 4.4 ns for $v = 4$, $N = 1$, and shorter for the energetically higher levels. By comparison, the purely radiative lifetime of the $i\,^3\Pi_g$ state is of the order of 15 ns.[5] Hence tunneling to the first excited dissociation limit is the dominant decay channel of the quasibound levels.

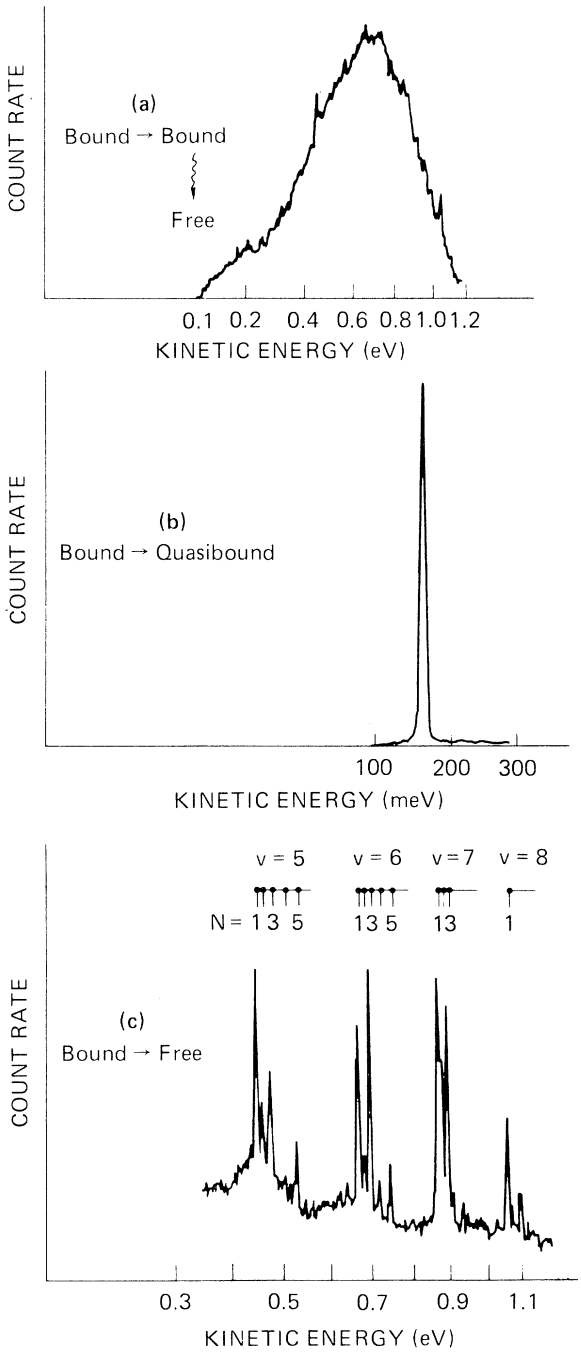

FIG. 3. Photofragment kinetic-energy spectra observed in photodissociation of H_2 $c\,^3\Pi_u^-$.

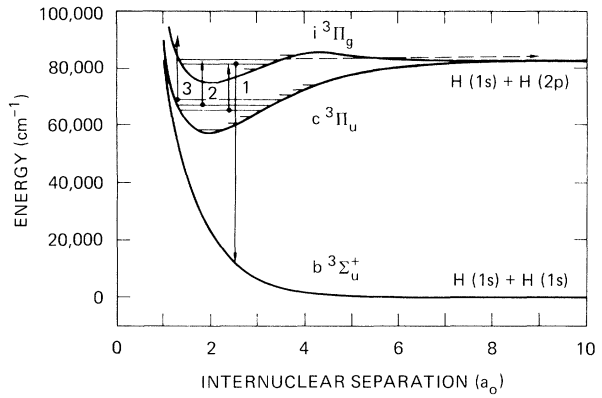

FIG. 4. Photodissociation channels from H_2 $c\,^3\Pi_u$: 1, bound-bound-free; 2, bound-quasibound; and 3, bound free.

(3) *Bound-free photodissociation.*—Underlying the discrete spectrum shown in Fig. 2 is a continuous background of laser-induced dissociation which arises from bound-free photodissociation. At a fixed laser wavelength, bound-free transitions will produce photofragments at energies $W = h\nu - D_{v,N}$, where $D_{v,N}$ is the dissociation energy of the rovibrational level with quantum numbers v,N from which the optical absorption occurs. Bound-free photodissociation at a fixed wavlength leads to a fragment energy distribution that reflects directly the lower-state rotational and vibrational spacings. Because of the very high energy resolution of the time- and position-sensitive detector we were able to resolve this distribution experimentally. Figure 3(c) shows such an energy distribution obtained at a fixed frequency near 16 480 cm^{-1}, where no noticeable peak occurs in the absorption spectrum. As indicated in this figure, bound-free transitions are observed from the vibrational levels $v'' = 5$, 6, 7, and 8 of the $c\,^3\Pi_u$ state, with individual rotational levels being resolved in the kinetic-energy spectrum. The intensity distribution over the individual rovibrational bound-free transitions reflects the population in the lower-state levels multiplied by the v- and N-dependent photodissociation cross section.

We have shown that a time- and position-sensitive detector can be used in photofragment spectroscopy in a fast neutral beam, allowing high-resolution absorption spectroscopy and translational energy spectroscopy on electronic molecular states that are coupled to the continuum. With this device we were able to investigate the bound, quasibound, and continuum vibrational levels of the $i\,^3\Pi_g$ state of H_2 in the vicinity of its dissociation limit $H(1s) + H(2p)$.

We acknowledge technical support by H. Pape and L. De Boer and fruitful discussions with Dr. T. R. Govers. This work is part of the research program of the Foundation for Fundamental Research on Matter (FOM). It was made possible by financial support of ZWO and also the National Science Foundation through Grants No. PHY 81-12548 and No. 84-11517.

[a]Permanent address: Molecular Physics Department, SRI International, Menlo Park, Cal. 94025.

[1]D. P. de Bruijn and J. Los, Rev. Sci. Instrum. **53**, 1020 (1982).

[2]D. P. de Bruijn, J. Neuteboom, and J. Los, Chem. Phys. **85**, 233 (1984).

[3]D. P. de Bruijn, J. Neuteboom, V. Sidis, and J. Los, Chem. Phys. **85**, 215 (1984); V. Sidis and D. P. de Bruijn, Chem. Phys. **85**, 201 (1984).

[4]C. E. Johnson, Phys. Rev. A **5**, 1026 (1972); R. P. Freis and J. R. Hiskes, Phys. Rev. A **2**, 573 (1970).

[5]E. E. Eyler and F. M. Pipkin, Phys. Rev. Lett. **47**, 1270 (1981).

[6]E. E. Eyler and F. M. Pipkin, J. Chem. Phys. **77**, 5315 (1982), and Phys. Rev. A **27**, 2462 (1983).

[7]*Hydrogen Molecule Wavelength Tables of Gerhard Heinrich Dieke,* edited by H. M. Crosswhite (Wiley-Interscience, New York, 1972).

[8]W. Kolos and J. Rychlewski, J. Mol. Spectrosc. **66**, 428 (1977).